Nature of Water Transport and Electro-Osmosis in Nafion: Insights from First-Principles Molecular Dynamics Simulations under an Electric Field

Yoong-Kee Choe,*,†,§ Eiji Tsuchida,†,§ Tamio Ikeshoji,†,§ Shunsuke Yamakawa,‡,§ and Shi-aki Hyodo‡,§

Research Institute for Computational Sciences (RICS), National Institute of Advanced Industrial Science and Technology (AIST), Centeral-2, Umezono 1-1-1, Tsukuba 305-8578, Japan, Toyota Central R&D Laboratories, Inc., Nagakute, Aichi, 480-1192, Japan, and CREST, Japan Science and Technology Corporation (JST), Honcho 4-1-8, Kawaguchi, Saitama 332-0012, Japan

Received: May 12, 2008

The effects of water content on water transport and electro-osmosis in a representative polymer electrolyte membrane, Nafion, are investigated in detail by means of first-principles molecular dynamics (MD) simulations in the presence of a homogeneous electric field. We have *directly* evaluated electro-osmotic drag coefficients (the number of water molecules cotransported with proton conduction) from the trajectories of the first-principles MD simulations and also *explicitly* evaluated factors that contribute to the electro-osmotic drag coefficients. In agreement with previously reported experiments, our calculations show virtually constant values (∼1) of the electro-osmotic drag coefficients for both low and high water content states. Detailed comparisons of each factor contributing to the drag coefficient reveal that an increase in water content increases the occurrence of the Grötthuss-like effective proton transport process, whose contribution results in a decrease in the electro-osmotic drag coefficient. At the same time, an environment that is favorable for the Grötthuss-like effective proton transport process is also favorable for the transport of water arising from water transport occurring beyond the hydration shell around the protons, whose contribution results in an increase in the electro-osmotic drag coefficient. Conversely, an environment that is not favorable for proton conduction is also not favorable for water transport. As a result, the electro-osmotic drag coefficient shows virtually identical values with respect to change in the water content.

I. Introduction

There is growing interest in polymer electrolyte membrane fuel cells (PEFCs) because of their potential applications in automobiles and small devices such as cellular phones. One of the key components of PEFCs is a polymer electrolyte membrane that facilitates proton conduction from the anode to the cathode. Nafion, a product of DuPont, is a representative polymer membrane exhibiting good proton conductivity as well as excellent chemical and mechanical stability.[1] Because of its significance in fuel cell development, Nafion has been extensively investigated.[2−20]

To obtain the maximum performance of PEFCs, the management of water is critical not only for effective proton conduction but also for the prevention of excess water localization at the cathode because of water transport.[21] It is believed that water transport in PEFCs occurs via electrochemical reactions at the anode (water consumed) and the cathode (water produced), the electro-osmotic drag of water by the proton−cotransport of water because of proton conduction−from the anode to the cathode and back diffusion of water from the cathode to the anode because of the water concentration gradient.[22] Electro-osmosis leads to the localization of water molecules in the vicinity of the cathode, which reduces the performance of fuel cells.[23,24] In spite of its significance in fuel cells, primarily because of the fact that complex experimental equipment is required, it has not been explored to the same extent as other chemical and physical properties affecting the performance of fuel cells.[23] Furthermore, while an electro-osmotic drag coefficient (the number of water molecules cotransported with proton conduction) is an important physical property that needs to be managed in PEFCs, it is one of the physical properties that is very difficult to rationalize.[25] The reasons may be the following. As previous experiments indicate, it is believed that an increase in water content inside Nafion increases the possibility of the Grötthuss-like structural diffusion of protons in the membranes. Because pictorial information on the Grötthuss mechanism[26] suggests that proton transport and water motion is decoupled, it is natural to reason that at higher water content, the value of the electro-osmotic drag coefficient is likely to be small. On the other hand, at lower water content, where proton transfer is believed to occur via the vehicular mechanism in which protons (H^+) migrate as H_3O^+, i.e., as bonded to a "*vehicle*" H_2O[27] (though we showed in a previous paper that this idea is not correct[28]), it is expected that proton conduction and water diffusion is strongly coupled, leading to a large electro-osmotic drag coefficient because H_3O^+ forms very strong hydrogen bonds with neighboring water molecules.[29] However, what is actually observed in experiments is that the values of the electro-osmotic drag coefficients are rather constant (∼1.0 according to the experiment of Zawodzinski et al.[25]) over a wide range of water content. Such a result apparently contradicts the above presumption based on the difference in the proton conduction mechanisms, which, in turn, raises a question regarding its origin. An earlier study employing a classical molecular

* Corresponding author. E-mail: yoongkee-choe@aist.go.jp.
† Research Institute for Computational Sciences (RICS), National Institute of Advanced Industrial Science and Technology (AIST).
‡ Toyota Central R&D Laboratories, Inc.
§ CREST, Japan Science and Technology Corporation (JST).

10.1021/jp8041878 CCC: $40.75 © 2008 American Chemical Society
Published on Web 08/22/2008

SCHEME 1: Schematic Illustration of Cation Conduction in an Aqueous Environment[a]

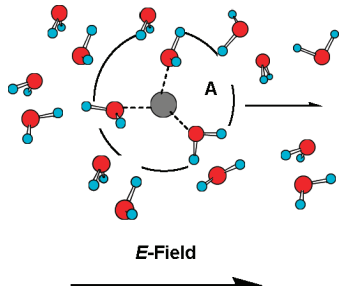

[a] Water transport occurring in region "**A**" is regarded as J_{H_2O}(hydration) while water transport occurring out of region "**A**" is regarded as J_{H_2O}(pumping). The black circle denotes a cation.

dynamics method produced electro-osmotic drag coefficients that are too large (~8−20), which may prevent one from drawing reasonable conclusions regarding the problem.[30]

In addition to the water transport affected *directly* by the nature of proton conduction, what causes the nature of the electro-osmosis in Nafion to be more complicated is details of water transport occurring beyond the hydration shell around the protons, a phenomenon that is also referred to by the term "hydrodynamic pumping" in the literature,[31,32] which is vague because of the difficulty experiments have in accurately probing the effect.[31] In general, conduction of cations through the membranes induces water transport accompanying it.[32] The water flux J_{H_2O} resulting from the transport of cations can be decomposed into the following terms:

$$J_{H_2O} = J_{H_2O}(\text{hydration}) + J_{H_2O}(\text{pumping})$$

where the first term arises from transport of water molecules that are *directly* bound to cations and the second term arises from the transport of water molecules occurring beyond the hydration shell,[32] whose details are described in Scheme 1. The water transport occurring in the circle "**A**" induces J_{H_2O}(hydration) and that occurring outside "**A**" induces J_{H_2O}(pumping). A general trend is that the contribution of the former is very large for metal cations with a small ionic radius such as Li^+ or Na^+, and the contribution of the latter is dominant for hydrophobic cations with a large ionic radius such as ammonium derived cations with bulky substituents.[31] However, unambiguous discrimination of the above two terms for proton conduction is experimentally very difficult,[31] a situation that calls for a contribution from sophisticated molecular simulations.

The present contribution is a continuation of our previous study where we treated the nature of proton conduction in Nafion[28] and demonstrated that in contrast to the general concept of the vehicular mechanism, proton hopping occurs with similar probability in the membranes with both low and high water content. Because the conduction of protons in an aqueous environment occurs with a completely different scheme compared with other cations, the water transport accompanying it in Nafion inevitably reflects the complex nature of the proton conduction. As will be shown later, water transport and electro-osmosis in Nafion are strongly affected by the nature of proton conduction, a situation that requires an accurate description of the proton shuttling mechanisms. As such, the use of a first-principles MD technique is highly desirable to capture the essence of the phenomena. Furthermore, inclusion of the electric field effect, in addition to the use of the first-principles MD technique, is necessary to compute an electro-osmotic drag coefficient and relevant properties.

SCHEME 2: Schematic Illustration of Modeled Nafion

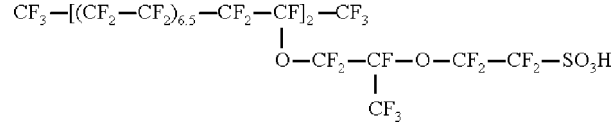

TABLE 1: Summary of Simulation Conditions

	conditions	
	L-state	*H-state*
molecule numbers in a unit cell		
N_{Nafion}	2	2
N_{H_2O}	13	47
$N_{H_3O^+}$	4	4
water content λ		
$(N_{H_2O} + N_{H_3O^+})/N_{SO_3^-}$	4.25	12.75
size of unit cell		
x/Å	12.3042	12.3042
y/Å	12.3042	12.3042
z/Å	28.1239	35.1549

Here, we present results of first-principles MD simulations under a homogeneous electric field carried out to investigate water transport and electro-osmosis in Nafion under several different conditions.

II. Computational Details

To obtain reasonable initial configurations for the use of the first-principles MD simulations, we started by carrying out classical MD calculations. Nafion was modeled as a polymer consisting of two monomers, as described in Scheme 2. Because a computation of the entire Nafion structure including cylindrical channels of water clusters[33] with the first-principles MD is not possible, we examined the basic sandwich structure consisting of the water region with hydrophilic side chains and surrounding hydrophobic regions. The MD simulations were carried out in a periodic three-dimensional cell, in which Nafion and water were stacked in the z-direction. Models with two different water contents were examined. The lattice constants of the x- and y-axes were fixed in order to represent the surface area of the micelle that was occupied by each sulfonic acid end group.[34] The lattice constant of the z-axis was determined in order to represent the composite density of dry Nafion[35] and water at a temperature of 363 K. The molecular numbers and the lattice constants of unit cells in the models are listed in Table 1. In the present study, two humidity levels, water content (λ = number of water molecules/number of sulfonic acid groups) equal to 4.1 and 12.7, were considered and hereafter we call the former the *L-state* (*low water content state*) and the latter the *H-state* (*high water content state*). Fujitsu Materials Explorer 3.0 was used for this simulation, which was performed assuming the *NVT* ensemble at 363 K using the Nosé-Hoover thermostat.[36−38] The total simulation time was approximately 200 ps with a time step of 0.2 fs. The proton that originated from the sulfonic acid end group was treated as a hydrated ion (H_3O^+). H_2O and H_3O^+ molecules were treated using the extended simple point charge (SPCE) water model.[39] The Dreiding force field[40] was adopted for all of the intramolecular potential forces of Nafion. Universal force field (UFF)[41] parameters were used to model the nonbonded interactions between H_2O (H_3O^+) and Nafion. The point charge present on each atom was determined by the electrostatic potential (ESP) method after molecular orbital calculations.[42] Snapshots of the simulated final configurations of Nafion/water complexes are shown in Figure 1. The

TABLE 2: Comparison of Average Velocity, Concentration, Flux, and Electro-Osmotic Drag Coefficients[a]

humidity (λ)	V_{H^+}	C_{H^+}	J_{H^+}	V_{H_2O}	C_{H_2O}	J_{H_2O}	$\varepsilon = (J_{H_2O}/J_{H^+})$
12.7 (*H-state*)	1.72×10^2	1.25	2.15×10^5	12.4	1.59×10^4	1.97×10^5	1.23
4.1 (*L-state*)	1.27×10	1.56	1.98×10^4	3.67	6.63×10^3	2.44×10^4	0.92

[a] V_X denotes the average velocity of X in m/s, C_X denotes the concentration of X in mol/dm^3, J_X denotes the flux (*velocity multiplied by concentration*) of X in mol m^{-2} s^{-1}, and ε is the electro-osmotic drag coefficient.

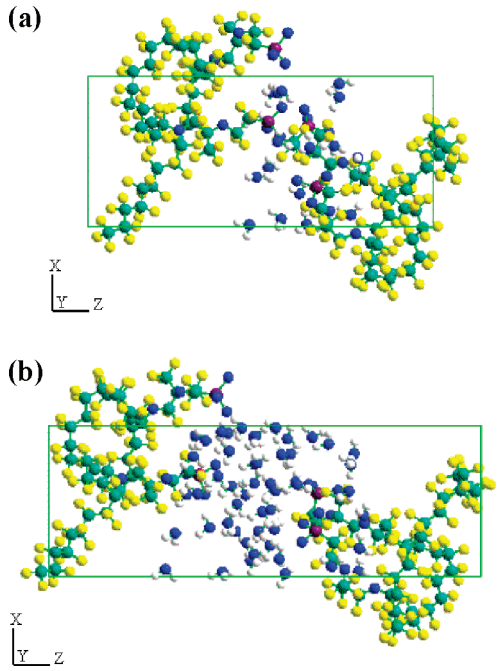

Figure 1. Snapshots of the configurations of (a) *L-state* and (b) *H-state*. Different atom types are denoted by different colors as follows: blue, oxygen; white, hydrogen; yellow, fluorine; green, carbon; and purple, sulfur.

hydrophilic side chains were oriented toward the water region, and thus, the two-phase structure was maintained.

Then, using the configurations obtained from the classical MD simulation as an initial configuration, first-principles MD simulations were performed. The electronic structures of the systems were evaluated by means of density functional theory in the Kohn−Sham formalism.[43,44] We used the generalized gradient approximation in the Perdew−Burke−Ernzerhof (PBE) form,[45] which is expected to give an accurate description of the hydrogen bonds.[46] Separable norm-conserving pseudopotentials[47−49] were employed, and only the Γ point was used to sample the Brillouin zone. Adaptive finite elements[50,51] were used in place of ordinary plane waves for the basis set. All production runs in the present paper were performed with an average cutoff energy of 57 Ry, while the resolution was approximately doubled at the positions of fluorine and oxygen atoms by adaptation of the grids.[52] In the molecular dynamics part, the nuclei were treated classically, and their equations of motion were integrated using the velocity-Verlet algorithm with the forces calculated from the electronic structure. The temperature was controlled by the Berendsen thermostat[53] with a target temperature of 353 K. All hydrogen atoms in the system were given the mass of deuterium to allow the use of a large time step of 1.21 fs in the production run. However, the deuterium atoms are denoted by H in the following analysis whenever there is no possibility of confusion. During the molecular dynamics simulations, the electronic states were quenched to the Born−Oppenheimer surface at every time step with the limited-memory variant of the quasi-Newton method.[54]

SCHEME 3: Definition of the *Transferring Proton*

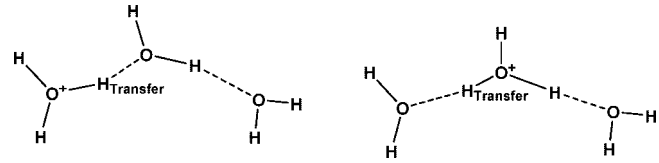

The wave functions were extrapolated from previous time steps.[55] First, equilibration runs up to 10 ps were carried out without an electric field and further simulations without an electric field were carried out up to 20 ps. Then, we performed simulations considering an electric field up to 10 ps. All of the calculations were carried out with our own finite element DFT code *FEMTECK* (finite element method-based total energy calculation kit). The above method has been successfully applied to liquid molecular systems.[56−59] The electric field was evaluated using the Berry phase theory, which is most appropriate for treating disordered systems under periodic boundary conditions.[60,61] We applied an electric field of 0.5 V/nm along the *x*-direction of the cells to achieve acceptable statistical accuracy at reasonable computational cost, while avoiding noticeable changes in liquid structures. Unless otherwise mentioned, all of the data and analysis presented were obtained from the trajectories of the first-principles MD including the effect of an electric field.

To evaluate the dynamical properties of protons (positive charge defects), we need to identify the coordinates of the protons. For this purpose, we define a *transferring proton* ($H_{transfer}$). As seen in Scheme 3, the *transferring proton* is one that is transferred to an adjacent water molecule by proton hopping. When a proton jump occurs, we can identify the Cartesian coordinate of the *transferring proton* and we can also identify the Cartesian coordinate of its position in a hydronium ion before the proton jump occurs.

The mean displacement of atoms, a quantity that will be used frequently in later sections, is obtained from Mean Dis. $= \langle \bar{r}_i(\tau) - \bar{r}_i(0) \rangle$ where $\bar{r}_i(\tau)$ is the position of atom i, τ is a time interval, and $\langle x \rangle$ is the average of a quantity x.

III. Results

A. Structural Features and Electric Field Effects. To investigate the nature of water transport, we first calculated the radial distribution functions (RDFs). Figure 2a shows RDFs for an atomic pair between O_w and the oxygen atom of the sulfonate group, where O_w denotes the oxygen atom of H_2O or H_3O^+. The first peak, located around 2.7 Å in Figure 2a, represents the first hydration shell around the sulfonate group. It is seen that the contribution of this peak depends on the water content. The number of water molecules (including hydronium ions) hydrating the sulfonate group directly is slightly larger in the *H-state*, as shown by integration of the RDF. However, because the number of water molecules in the cell is much smaller in the *L-state*, it follows that a larger fraction of water molecules is participating in the hydration of the sulfonate group compared with the *H-state*. This fact also indicates that a large fraction of water molecules in the *L-state* is strongly affected

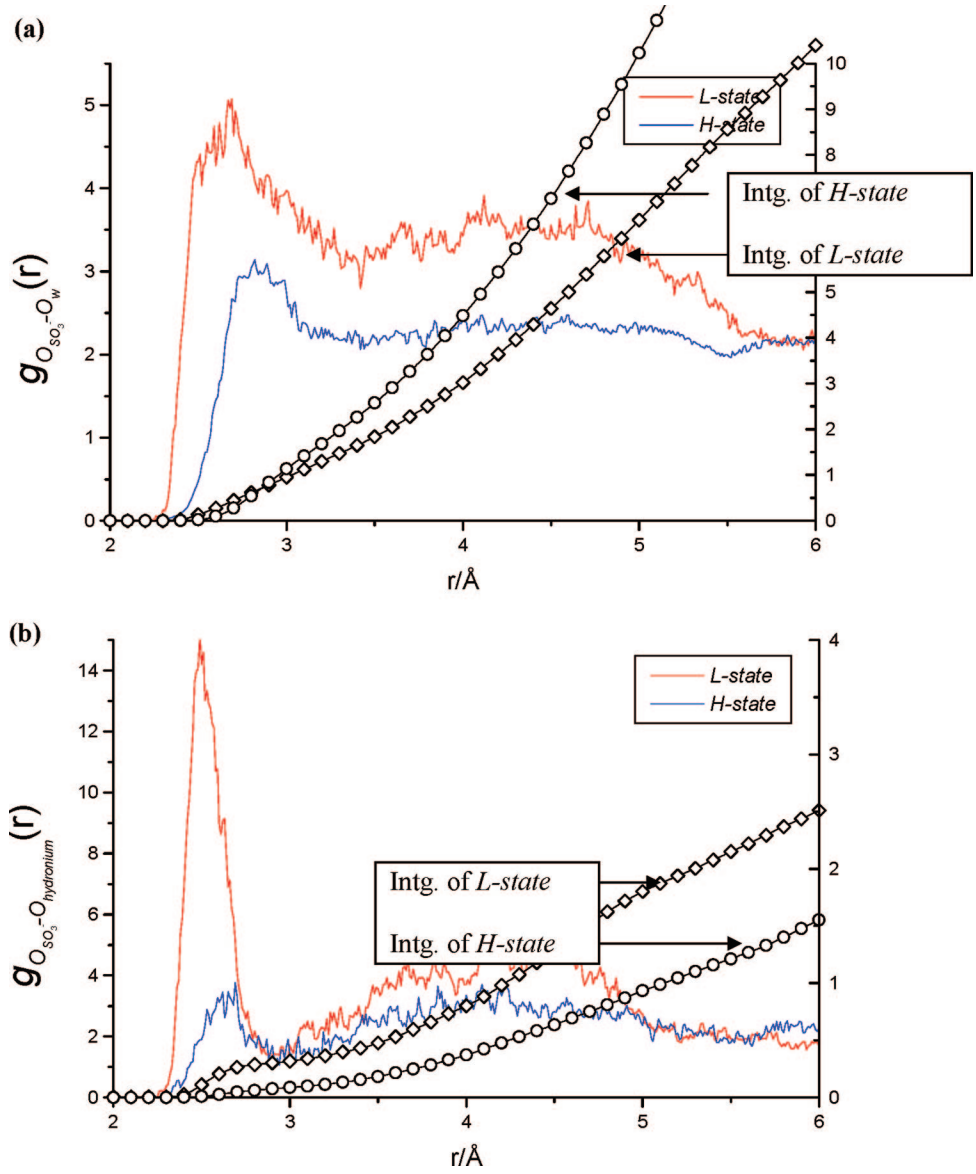

Figure 2. (a) Radial distribution function (RDF) for an atomic pair between the oxygen atom of SO_3^- and that of water and hydronium ion (O_w). (b) An RDF for an atomic pair between the oxygen atom of SO_3^- and that of hydronium ions. In addition to the RDFs, we also plotted the integrals of the functions, whose values are shown in the right *y*-axis.

by the negative charge of the sulfonate oxygen, whose effect tends to slow down the diffusion of water molecules around the sulfonate group.[62] In Figure 2b, we present RDFs for an atomic pair between the oxygen atom of hydronium ions and the oxygen atom of the sulfonate group, for comparison. The first peak is located around 2.5 Å, which implies short and strong hydrogen bonds between the hydronium ion and the sulfonate oxygen. Integration of the RDF shows that the number of hydronium ions located next to the sulfonate group is larger in the *L-state* than in the *H-state*. The very large contribution of the first peak in the *L-state* indicates that the proton transport mechanism is not operating effectively in the *L-state.* In contrast, the contribution of the first peak is very small and less structured in the *H-state*. Such a feature is different from the RDF for the same atomic pair obtained by a classical molecular dynamics simulation, which shows a rather structured feature even in the high water content state.[12] The difference between the classical and the first-principles results may arise from the difficulty of the classical molecular dynamics simulation in modeling the Grötthuss-type structural diffusion.

In Figure 3a, a comparison of the RDFs for the atomic pair between sulfonate oxygen atom and O_w ($H_2O + H_3O^+$) with and without the inclusion of the electric field is presented. The effect of the electric field is very minor for such a pair. The RDFs for the atomic pair between the sulfonate oxygen atom and the oxygen atom of hydronium ions are presented in Figure 3b. While the features of the RDFs shown in Figure 3b are changed upon the application of the electric field, as shown in Figure 3a, its effect is very marginal for the structural features related to the whole O_w distribution.

B. Dynamical Property. In Figure 4, we present the *x* component of four *transferring protons* and its average. The average value of the *x* component shows that its value is changed gradually as the simulation time step is increased. However, the movement of the individual protons shows that the movement in the *x* direction is not continuous. For example, as shown in Figure 4 (b) "*proton 4*" in the *H-state* is relatively immobile up to 5000 fs, and after 5000 fs it moves in the *x* direction in a rather consecutive manner. In the *L-state*, as shown in Figure 4 (a), "*proton 2*" shows a significant movement in the *x* direction

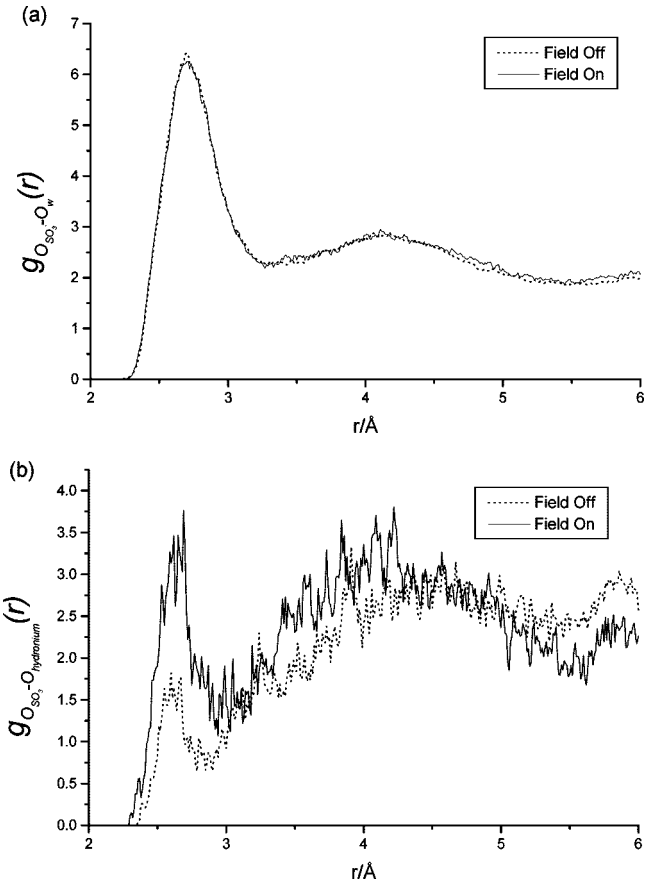

Figure 3. (a) RDFs for an atomic pair between the oxygen atom of SO_3^- and that of water and hydronium ion (O_w) with and without the inclusion of the electric field. (b) RDFs for an atomic pair between the oxygen atom of SO_3- and that of hydronium ions with and without the inclusion of the electric field. All of the RDFs were evaluated from the trajectories of the *H-state*.

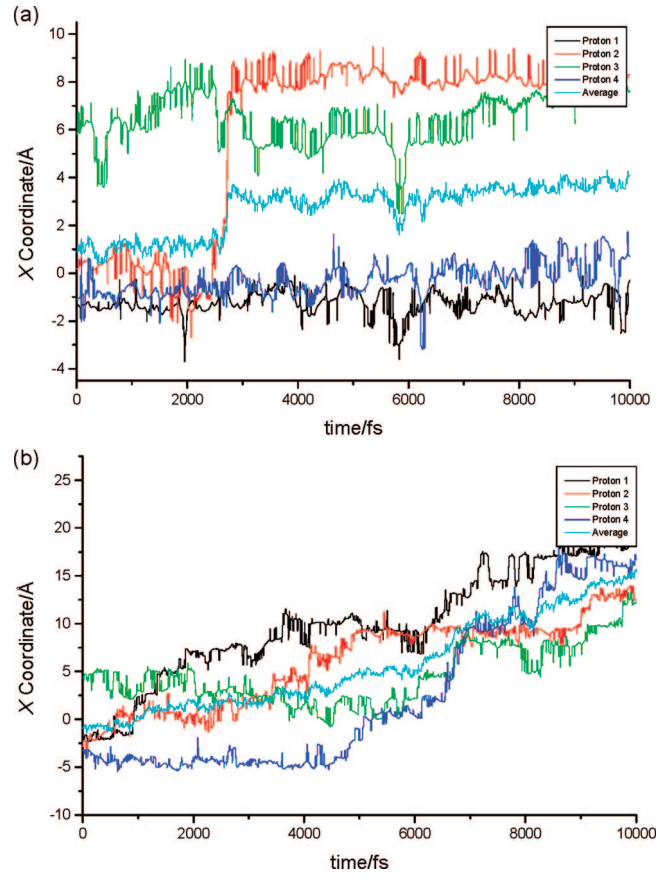

Figure 4. Change of the *x* component of the *transferring protons* and their average as a function of time: (a) *L-state*; (b) *H-state*.

compared to other three protons. The change in the average value for the four protons in the *L-state*, thus mostly arises from the consecutive proton jump of "*proton 2*", occurring at around 2500 fs.

Figure 5 shows a comparison of mean displacement of O_w and H_w where H_w denotes hydrogen atoms of H_2O or H_3O^+. When molecules containing an O_w atom form a charged species such as H_3O^+, it should move in the direction of the applied electric field as a response to the electric field. Because we applied the electric field to the *x*-direction of the simulation cell, we only show the change in the *x* component of the Cartesian coordinate. The slope of the plots is the rate of change of displacement, which equals the mean velocity ($\bar{v}$). The mobility, which is calculated from *u*(mobility) $= \bar{v}/E$ where *E* denotes the applied electric field, of O_w is 0.7×10^{-4} and 2.4×10^{-4} $cm^2\ s^{-1}\ V^{-1}$, for the *L*- and *H-states*, respectively. The mobility of O_w in the *L-state* is smaller than that in the *H-state*, as expected. In Figure 5, it is notable that the difference of the slopes between O_w and H_w is very small in the *L-state* compared with that in the *H-state*. The result, in accord with the analysis of the RDFs, implies that a proton transport process in the *L-state* is effectively not functioning,[28] resulting in the similar mean velocities of the O_w and H_w atoms. On the other hand, in the *H-state*, the difference in the slopes is larger, indicating that a more effective proton transport process is operating. That is, the result suggests that in the *H-state* the protons diffuse more independently of the water molecules than in the *L-state*.

Comparing the slope of O_w for the *L-state* and the *H-state*, it is noted that the slope of the *H-state* is steeper than that of the *L-state*. One of the reasons for such a difference comes from the fact that in the *L-state*, 43% of water molecules are, on average, within the first hydration shell, while the ratio in the *H-state* is 16%, values that are obtained from integration of the RDFs shown in Figure 2. In Figure 6, we present the local displacement of the O_w atom for the *H-state*, where statistics are collected for O_w atoms residing within 4.0 Å of the sulfonate sulfur atoms (indicated as Inner) and O_w atoms residing 4.0 Å away from all of the sulfonate sulfur atoms (indicated as Outer). It is seen that O_w atoms located closer to the sulfonate group are moving more slowly. Thus, the result confirms that the large number of water molecules residing in the first hydration shell around the sulfonate group decreases the total mobility of the O_w atoms.

Now, we investigate details of the water transport from a different perspective, namely the nature of water transport occurring beyond the hydration shell. As addressed, water molecules in polymer electrolyte membranes containing cations are known to be transported as hydrating water molecules *directly* bound to cations or as pumped hydrodynamically by cations. Kreuer et al. have compared electro-osmotic drag coefficients of Nafion and sulfonated polyetherketones (PEEKK) and suggested that the difference in the electro-osmotic drag coefficients between the two membranes is contributed largely from effects of hydrodynamic pumping.[63] In the modified hydrodynamic model of Miller et al.,[32] which is introduced by

Kreuer et al. to consider the Grötthuss mechanism of the proton conduction, an electro-osmotic drag coefficient is expressed by:

$$\varepsilon = \frac{\Gamma_{\text{hydro}}}{\Gamma_{\text{hydro}} + \Gamma_{\text{trans}}}\left(n_{\text{hydro}} + (n - n_{\text{hydro}})\frac{\bar{v}_{\text{H}_2\text{O}}}{v_p}\right) \qquad (1)$$

where Γ_{hydro} is the rate for hydrodynamic transport of hydrated protons (i.e., movement of the hydronium ion itself), Γ_{trans} is the proton transfer rate (i.e., movement by the Grötthuss mechanism), v_p is the drift velocity of the hydrated protons, $\bar{v}_{\text{H}_2\text{O}}$ is the mean velocity of water molecules outside the proton hydration shell, n represents the number of whole water molecules per cation, and n_{hydro} denotes the number of water molecules hydrating the protons. The term $\Gamma_{\text{hydro}}/(\Gamma_{\text{hydro}} + \Gamma_{\text{trans}}) = h$ in eq 1 is indicative of the effectiveness of the proton transport mechanism. The smaller the value of h, the more effective will be the proton transport process. The denominator $(\Gamma_{\text{hydro}} + \Gamma_{\text{trans}})$ represents the velocity of protons (positive charge defect), which is evaluated from the graphs presented in Figure 7 where we plot time evolution of the displacement of the protons (positive charge defects). The numerator corresponds to the velocity of the protons that is obtained by excluding the contribution of proton jumping, a value that can be evaluated from the graphs shown in Figure 8, where we present the time evolution of the hydronium ion's displacement. The hydronium ion is defined if O_w atoms reside within 1.2 Å from the *transferring protons* and the O_w atoms that are not assigned as a hydronium ion's O_w are considered to be water molecules residing outside the hydration shell. Linear fits were made for the curves whose x values lie in the range 0−30 fs. Note that in our previous study,[28] we demonstrated that proton hopping in Nafion occurs with a rate of 4−5 times per 100 steps (one step = 1.21 fs) both in the *L-state* and the *H-state*. Thus, the lifetime of a hydronium ion is about 20−30 fs. The values of h are calculated to be 0.69 and 0.24 for the *L-state* and the *H-state*, respectively. Obviously, the smaller h value in the *H-state* is an indication of the effective proton transport process occurring in the *H-state*.

The term $p = (n\text{-}n_{\text{hydro}})\bar{v}_{\text{H}_2\text{O}}/v_p$ in eq 1 stands for the contribution of the transport of water molecules that are dragged by proton conduction but not participating in the hydration of protons. Thus, the larger the value of p, the larger will be the contribution of the transport of water occurring beyond the hydration shell. Figure 8 shows plots of time evolution of displacement for hydronium ions and water molecules residing outside the hydration shell. $\bar{v}_{\text{H}_2\text{O}}/v_p$ can be evaluated from the ratio of the slopes of the plots shown in Figure 8. It is seen in Figure 8 that $\bar{v}_{\text{H}_2\text{O}}$, the velocity of water molecules residing outside the hydration shell, is smaller in the *L-state* than in the *H-state* and the velocity of hydronium ions is rather similar for both states. In our systems, the value of $\bar{v}_{\text{H}_2\text{O}}/v_p$ is calculated to be 0.10 and 0.26 and the term p is then calculated to be 1.3 and 4.1 for the *L-state* and the *H-state*, respectively. The contribution of water transport occurring beyond the hydration shell is more dominant in the *H-state* than in the *L-state*, an effect that appears completely opposite to the trend in the h term. Therefore, in the *H-state,* the h term is small and the p term is large, while the trend in the *L-state* is completely the opposite, all of which results in the rather similar electro-osmotic drag coefficients.

IV. Discussion

Table 2 summarizes the computed drag coefficients and related data. The values in Table 2 are evaluated using the definition of the electro-osmotic drag coefficient, which is expressed as $\varepsilon = J_{\text{H}_2\text{O(O}_w\text{)}}/J_{\text{H}^+}$ ($J_X = v_X c_X$, where v_X denotes the mean velocity of X, and c_X denotes the concentration of X and is equivalent to eq 1). The calculated electro-osmotic drag coefficients are 0.92 and 1.23 for the *L-* and *H-states*, respectively. The result agrees satisfactorily with the experiment of Zawodzinski et al.[25] whose result also shows that, over a wide range (λ = 1.4−14), the electro-osmotic drag coefficients are about 1.0.[64]

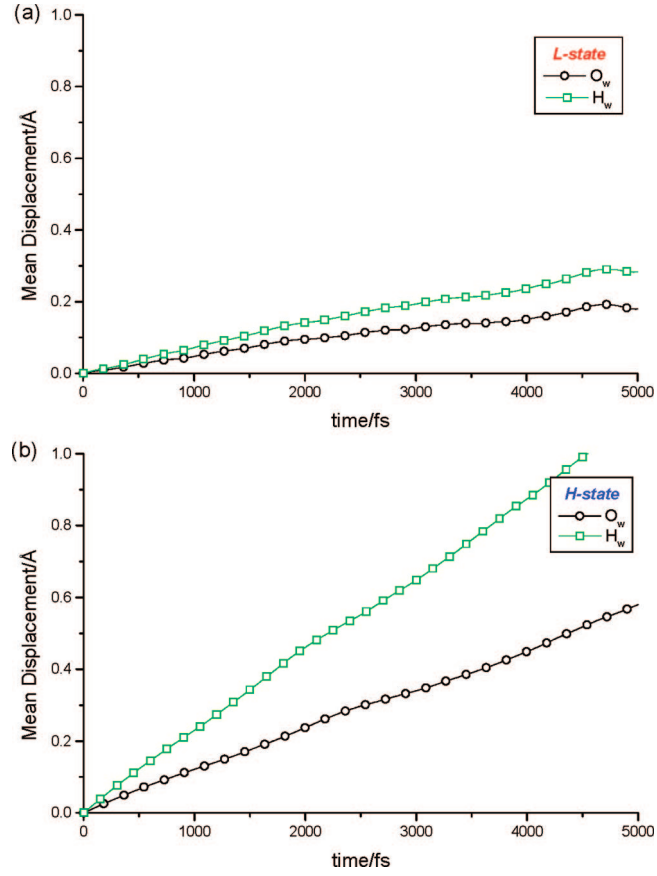

Figure 5. Plots of mean displacement vs time for O_w and H_w atoms for (a) *L-state* and (b) *H-state.*

As mentioned in the above section, proton transfer occurs more effectively in the *H-state* than in the *L-state*. In our previous paper, we demonstrated that the proton hopping probability is almost independent of the water content.[28] In other words, even in the *L-state*, where it is believed that proton conduction occurs in a vehicular manner, proton hopping occurs with a nonnegligible rate that is comparable with that in the *H-state*. Thus, the description of proton conduction derived from the idea of the vehicular mechanism does not correctly provide atomistic details of the proton motion. Instead, we have proposed that proton conductivity in Nafion can be explained by the ratio of the *constructive* and the *nonconstructive* proton transfer events. Details of the *constructive* and the *nonconstructive* proton transfer are shown in Scheme 4. The *constructive* proton transfer is, as defined, the transfer of a proton that moves further away from its original position. On the other hand, the *nonconstructive* proton transfer is the transfer of a proton that comes to the position of the oxygen site of the original water in the end. An increase in the occurrence of the *constructive* proton transfer increases the proton conductivity. A key factor that determines the ratio between the *constructive* proton transfer and the *nonconstructive* proton transfer events is the hydrogen-bond network of the water molecules. As the previous classical molecular dynamics simulations[17] as well as our previous

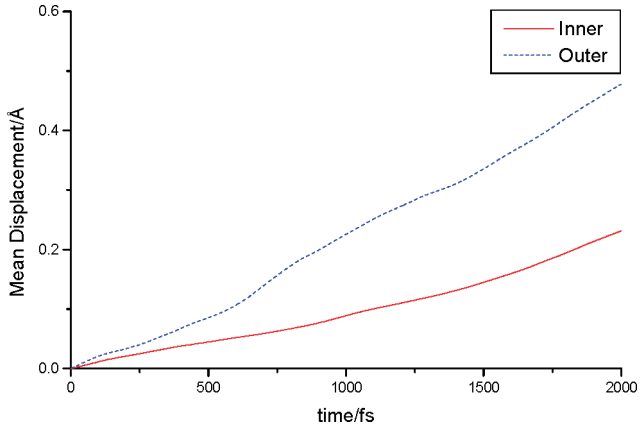

Figure 6. Plots of mean displacement vs time for O_w atoms of the *H-state*. The "Inner" plot indicates the displacement of O_w atoms residing within 4.0 Å of the sulfonate sulfur atoms and "Outer" plot indicates the displacement of O_w atoms residing 4.0 Å away from all of the sulfonate sulfur atoms.

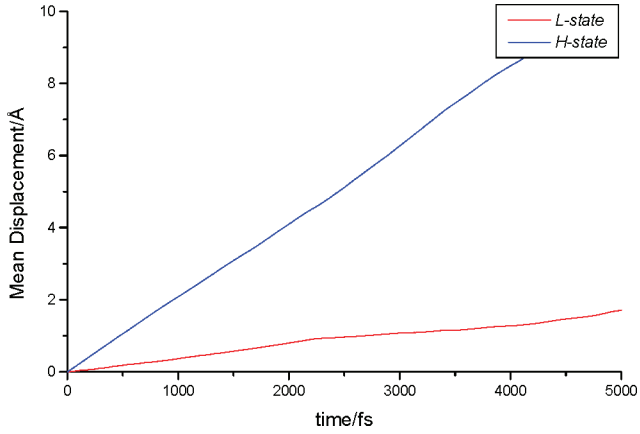

Figure 7. Plots of mean displacement vs time for protons (positive charge defects).

results[28] on Nafion demonstrate, the water molecules in the *L-state* form a cluster structure where the hydrogen-bond network of water molecules is rather discontinuous while it is very continuous to exhibit a bulk-like structure in the *H-state*.

The continuous and bulk-like hydrogen-bond network of water molecules allows for proton transfer to occur in a manner that *constructively* contributes to proton conduction and the increase in its contribution enhances the proton conductivity. This effect is reflected in the *h* term shown in eq 1 and tends to reduce the electro-osmotic drag coefficients. On the other hand, in the environment where water molecules form small water clusters, the contribution of proton transfer occurring in a *nonconstructive* manner is increased, an effect that appears to increase the electro-osmotic drag coefficient, giving a larger value for the *h* term compared with that for the *H-state*. Thus, just considering the proton transfer details, it is very likely that the electro-osmotic drag coefficient is larger in the *L-state* than in the *H-state*, as we speculated in the Introduction. However, such an environment where proton conduction occurs effectively also enhances the mobility of water. As the difference in the *p* term indicates, the transport of water molecules occurring beyond the hydration shell is also dependent on the water content. Its effect is more dominant in the *H-state* than in the *L-state* and tends to increase the electro-osmotic drag coefficients. In the bulk-like continuous water hydrogen-bond network, water transport occurring in one area of the network influences other water molecules in the network through the

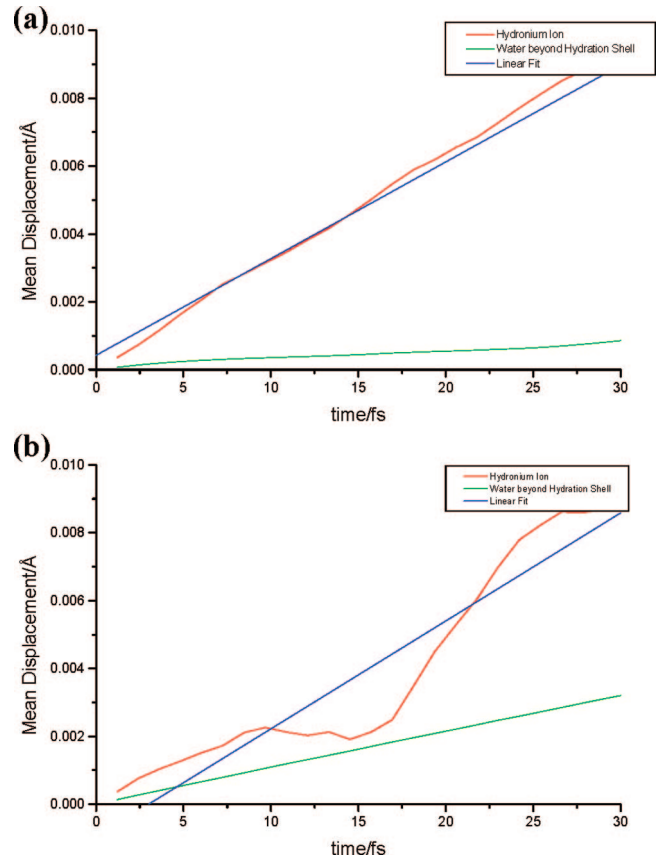

Figure 8. Plots of mean displacement vs time for hydronium ions, water molecules (O_w) residing outside the hydration shell and linear fit for the plot on hydronium ion's mean displacement for (a) *L-state* and (b) *H-state*.

SCHEME 4: Proton Transfer[a]

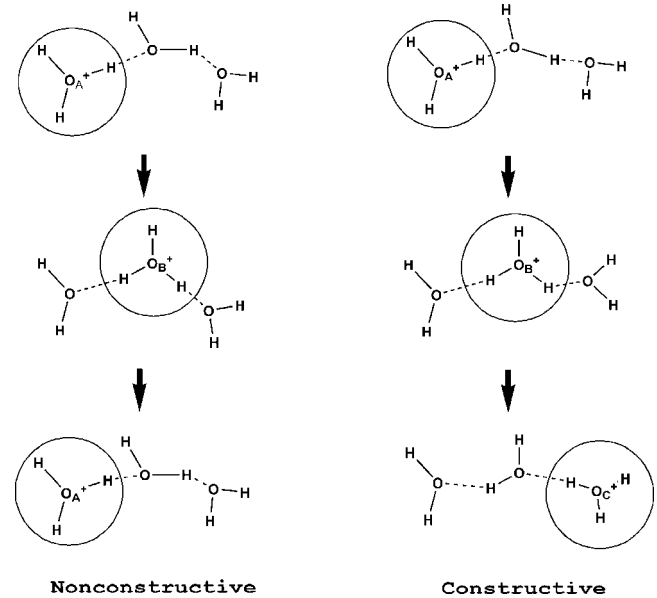

[a] Constructive proton transfer is the transfer of a proton that moves further away from its original location. Nonconstructive proton transfer is the transfer of a proton that comes to the position of the oxygen site of the original water in the end. The contribution to proton conduction is larger in the former and smaller in the latter.

hydrogen bonding. On the other hand, in the environment where the water hydrogen-bond network is disconnected forming many cluster structures, even if water transport occurs, its effect on

other water molecules should be less influential compared with that in the bulk-like environment. As such, in the *H-state*, the water transport residing beyond the hydration shell around protons is more effective than in the *L-state*.

As discussed above, proton hopping occurs at a rate of about 4−5% during the simulations, which means that the proton hopping occurs about 4−5 times during 100 simulation time steps, implying that protons spend most of the time as hydrated species such as H_3O^+ regardless of water content. A hydronium ion should drag at least one water molecule as its morphology indicates and therefore the proton conduction occurring because of conduction as H_3O^+ can be regarded as the proton conduction that drags water molecules. Moreover, the electro-osmotic drag coefficient can be larger than one if the contribution of proton conduction through the effective proton hopping is neglected and one considers the number of water molecules hydrating the hydronium ion. The number of water molecules hydrating the hydronium ion is 3.0 and 2.0 for the *H-state* and *L-state*, respectively.[65] Such a result also explains why $\bar{v}_{H_2O}$ (velocity of the water molecules residing outside the hydration shell) that is evaluated from the plots in Figure 8 is smaller in the *L-state* than in the *H-state* because the number of water molecules directly hydrating H_3O^+ is smaller in the *L-state*. Therefore, just considering the hydronium ion's hydration, the *H-state* is more favorable for dragging water molecules (obviously, the value of the electro-osmotic drag coefficients cannot be as large as 2 or 3 because of the contribution of the proton conduction that does not drag water molecules). The account in this manner could be a reinterpretation of the data and analysis in the previous section and highlights that the previously proposed idea on the proton transport in Nafion based on the Grötthuss/Vehicular mechanism is oversimplified (although it can explain some but not all experimental observations to a certain degree) and does not provide a proper description of electro-osmosis. As we addressed in the Introduction, the previously proposed idea gives a description where in the *L-state*, proton transport occurs as H_3O^+, whose conduction may drag many water molecules compared with the conduction in the *H-state*. However, in contrast to the speculation, the contribution of the drag of water molecules by H_3O^+ is more dominant in the *H-state* than in the *L-state*, in contradiction of the previously proposed idea.

V. Concluding Remarks

In the present study, we have applied first-principles MD including the effect of an electric field to investigate the nature of water transport and electro-osmosis in Nafion. We *explicitly* estimated several factors contributing to the electro-osmosis from the trajectories of the simulations. Our study, as far as we know, provides for the first time detailed values of the elements that contribute to an electro-osmotic drag coefficient. Because proton conduction depends on the water content, water transport inside Nafion is found to depend strongly on the water content. Electro-osmotic drag coefficients, which require an accurate description of the proton and water diffusion process for its evaluation, were computed from the trajectories of the first-principles MD simulations in the presence of a homogeneous electric field. The obtained values are 0.92 and 1.23 for the low water content state and the high water content state, respectively. Our simulations revealed that proton conduction and water transport are strongly coupled. A good environment for the former is also a good environment for the latter and vice versa, resulting in the relatively constant electro-osmotic drag coefficients regardless of the water content. Finally, it must be emphasized that the previously proposed idea that accounts for the difference in the proton conduction in Nafion with respect to water content employing the Grötthuss/Vehicular concept does not provide a correct atomistic level description of the proton dynamics in Nafion, which prevents one from drawing reasonable conclusions about the electro-osmosis.

Acknowledgment. All calculations were performed at the AIST Super Cluster. The authors would like to acknowledge T. Ikeda for generating the pseudopotentials. This study was supported, in part, by the Nanoscience Program of the Next Generation Super Computing Project of the Ministry of Education, Culture, Sports, Science and Technology (MEXT), Japan.

References and Notes

(1) Mauritz, K. A.; Moore, R. B. *Chem. Rev.* **2004**, *104*, 4535.
(2) Kreuer, K.-D.; Paddison, S. J.; Spohr, E.; Schuster, M. *Chem. Rev.* **2004**, *104*, 4637, and references therein.
(3) Petersen, M. K.; Voth, G. A. *J. Phys. Chem. B* **2006**, *110*, 18594.
(4) Eikerling, M.; Kornyshev, A. A. *J. Electroanal. Chem.* **2001**, *502*, 1.
(5) Commer, P.; Harting, C.; Seeliger, D.; Spohr, E. *Mol. Simul.* **2004**, *30*, 755.
(6) Dokmaisrijan, S.; Spohr, E. *J. Mol. Liq.* **2006**, *129*, 92.
(7) Spohr, E.; Commer, P.; Kornyshev, A. A. *J. Phys. Chem. B.* **2002**, *106*, 10560.
(8) Petersen, M. K.; Wang, F.; Blake, N. P.; Metiu, H.; Voth, G. A. *J. Phys. Chem. B* **2005**, *109*, 3727.
(9) Seelinger, D.; Hartnig, C.; Spohr, E. *Electrochim. Acta* **2005**, *50*, 4234.
(10) Zawodzinski, T. A., Jr.; Derouin, C.; Radzinski, S.; Sherman, R. J.; Smith, V. T.; Springer, T. E.; Gottesfeld, S. *J. Electrochem. Soc.* **1993**, *140*, 1041.
(11) Cappadonia, M. J.; Erning, W.; Stimming, U. *J. Electroanal. Chem.* **1994**, *376*, 189.
(12) Cui, S.; Liu, J.; Selvan, M. E.; Keffer, D. J.; Edwards, B. J.; Steele, W. V. *J. Phys. Chem. B* **2007**, *111*, 2208.
(13) Schmidt-Rohr, K.; Chen, Q. *Nat. Mat.* **2008**, *7*, 75.
(14) Zhou, X.; Chen, Z.; Delgado, F.; Brenner, D.; Srivastava, R. *J. Electrochem. Soc.* **2007**, *154*, B82.
(15) Paddison, S. J.; Elliot, J. A. *J. Phys. Chem. A* **2005**, *109*, 7583.
(16) Brandell, D.; Karo, J.; Liivat, A.; Thomas, J. O. *J. Mol. Model.* **2007**, *13*, 1039.
(17) Devanathan, R.; Venkatnathan, A.; Dupuis, M. *J. Phys. Chem. B* **2007**, *111*, 13006.
(18) Jinnouchi, R.; Okazaki, K. *J. Electrochem. Soc.* **2003**, *150*, E66.
(19) Rowe, A.; Li, X. *J. Power Sources* **2001**, *102*, 82.
(20) Hofmann, D. W. M.; Kuleshova, L.; D'Aguanno, B. *J. Mol. Model.* **2008**, *14*, 225.
(21) Zawodzinski, T. A.; Neeman, M.; Sillerud, L. O.; Gottesfeld, S. *J. Phys. Chem.* **1991**, *95*, 6040.
(22) Eikerling, M.; Kharkats, Y. I.; Kornyshev, A. A.; Volfkavich, Y. M. *J. Electrochem. Soc.* **1998**, *145*, 2684.
(23) Pivovar, B. S. *Polymer* **2006**, *47*, 4194.
(24) Ren, X.; Gottesfeld, S. *J. Electrochem. Soc.* **2001**, *148*, A87.
(25) Zawodzinski, T. A.; Davey, J.; Valerio, J.; Gottesfeld, S. *Electro. Chim. Acta* **1995**, *40*, 297.
(26) Marx, D.; Tuckerman, M. E.; Hutter, J.; Parrinello, M. *Nature* **1999**, *937*, 601.
(27) Kreur, K.-D.; Rabenau, A.; Weppner, W. *Angew. Chem., Int. Ed. Engl.* **1982**, *21*, 208.
(28) Choe, Y.-K.; Tsuchida, E.; Ikeshoji, T.; Yamakawa, S.; Hyodo S. Submitted for publication.
(29) Markovitch, O.; Agmon, N. *J. Phys. Chem. A* **2007**, *111*, 2253.
(30) Din, X.-D.; Michaelides, E. E. *AIChE. J.* **1998**, *44*, 35.
(31) Xia, G.; Okada, T. *Electrochim. Acta* **1995**, *95*, 1569.
(32) Breslau, B. R.; Miller, I. F. *Ind. Eng. Chem. Fundam.* **1971**, *10*, 554.
(33) Gierke, T. D.; Mumn, G. E.; Wilson, F. C. *J. Polymer Sci. B: Polym. Phys.* **1981**, *19*, 1687.
(34) Dreyfus, B.; Gebel, G.; Aldebert, P.; Pineri, M.; Escoubes, M.; Thomas, M. *J. Phys. (Paris)* **1990**, *51*, 1341.
(35) Takamatsu, T.; Eisenberg, A. *J. Appl. Polym. Sci.* **1979**, *24*, 2221.
(36) Nosé, S. *Mol. Phys.* **1984**, *52*, 255.
(37) Nosé, S. *J. Chem. Phys.* **1984**, *81*, 511.
(38) Hoover, W. G. *Phys. Rev. A* **1985**, *31*, 1695.
(39) Berendsen, H. J. C.; Grigera, J. R.; Straatsma, T. P. *J. Phys. Chem.* **1987**, *91*, 6269.

(40) Mayo, S. L.; Olafason, B. D.; Goddard, W. A., III *J. Phys. Chem.* **1990**, *94*, 8897.

(41) Rappé, A. K.; Casewit, C. J.; Colwell, K. S.; Goddard, W. A., III.; Skiff, W. M. *J. Am. Chem. Soc.* **1992**, *114*, 10024.

(42) Singh, U. C.; Kollman, P. A. *J. Comput. Chem.* **1984**, *5*, 129.

(43) Hohenberg, P.; Kohn, W. *Phys. Rev.* **1964**, *136*, B864.

(44) Kohn, W.; Sham, L. J. *Phys. Rev.* **1965**, *140*, A1133.

(45) Perdew, J. P.; Burke, K.; Ernzerhof, M. *Phys. Rev. Lett.* **1996**, *77*, 3865.

(46) Tsuzuki, S.; Lüthi, H. P. *J. Chem. Phys.* **2001**, *114*, 3949.

(47) Kleinman, L.; Bylander, D. M. *Phys. Rev. Lett.* **1982**, *48*, 1425.

(48) Goedecker, S.; Teter, M.; Hutter, J. *Phys. Rev. B* **1996**, *54*, 1703.

(49) Hartwigsen, C.; Goedecker, S.; Hutter, J. *Phys. Rev. B* **1998**, *58*, 3641.

(50) Tsuchida, E.; Tsukada, M. *Phys. Rev. B* **1996**, *54*, 7602.

(51) Tsuchida, E.; Tsukada, M. *J. Phys. Soc. Jpn.* **1998**, *67*, 3844.

(52) Gygi, F. *Phys. Rev. B* **1995**, *51*, 11190.

(53) Berendsen, H. J. C.; Postma, J. P. M.; van Gusteren, W. F.; DiNola, A.; Haak, J. R. *J. Chem. Phys.* **1984**, *81*, 3684.

(54) Press, W. H.; Teukolsky, S. A.; Vetterling, W. T.; Flannery, B. P. *Numerical Recipes in FORTRAN*; Cambridge University Press: Cambridge, U.K., 1992).

(55) Arias, T. A.; Payne, M. C.; Joannopoulos, J. D. *Phys. Rev. Lett.* **1992**, *69*, 1077.

(56) Tsuchida, E. *J. Chem. Phys.* **2004**, *121*, 4740.

(57) Tsuchida, E. *J. Phys. Soc. Jpn.* **2006**, *75*, 054801.

(58) Choe, Y.-K.; Tsuchida, E.; Ikeshoji, T. *J. Chem. Phys.* **2007**, *126*, 154510.

(59) Choe, Y.-K.; Tsuchida, E.; Ikeshoji, T. *Comput. Phys. Commun.* **2007**, *177*, 38.

(60) Umari, P.; Pasquarello, A. *Phys. Rev. Lett.* **2002**, *89*, 157602.

(61) Souza, I.; Íñiguez, J.; Vanderbilt, D. *Phys. Rev. Lett.* **2002**, *89*, 117602.

(62) Blake, N. P.; Mills, G.; Metiu, H. *J. Phys. Chem. B* **2007**, *111*, 2490.

(63) Ise, M.; Kreuer, K. D.; Maier, J. *Solid State Ionics* **1999**, *125*, 213.

(64) A recent report by Yi et al. (*J. Electrochem. Soc.* **2006**, *153*, A1443) shows that an electro-osmotic drag coefficient is gradually increasing in going from the low water content state to the high water content state while the difference of the electro-osmotic drag coefficient between the low and high water content state is not so large.

(65) The coordination number regarding the water molecules around a hydronium ion is evaluated by integrating the first peak of the RDFs.

JP8041878